ELECTRONIC SUPPORTING INFORMATION

Slow Relaxation of Magnetization and Luminescence Properties of a Novel Dysprosium and Pyrene-1,3,6,8-tetrasulfonate Based MOF

Amalia García-García, Itziar Oyarzabal, Javier Cepeda, José M. Seco, Antonio A. García-Valdivia, Santiago Gómez-Ruiz, Alfonso Salinas-Castillo, Duane Choquesillo-Lazarte and Antonio Rodríguez-Diéguez

Index:

1. **Single Crystal X-ray Diffraction**
2. **Elemental analysis of pytet ligand**
3. **Continuous Shape Measurements**
4. **Powder X-ray Diffraction**
5. **FTIR analysis**
6. **Magnetic Properties**
7. **Photoluminescence Properties**

1. Single Crystal X-ray Diffraction

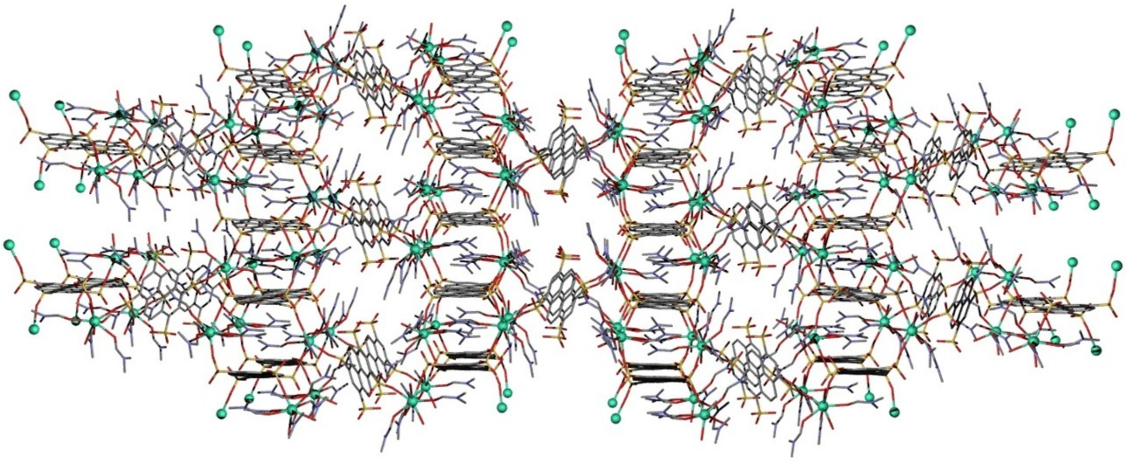

Figure S1. Perspective view of the packing of compound **1** showing small channels along *a* axis. Colour code: Dysprosium, green; oxygen, red; nitrogen blue; carbon, black; hydrogen, white.

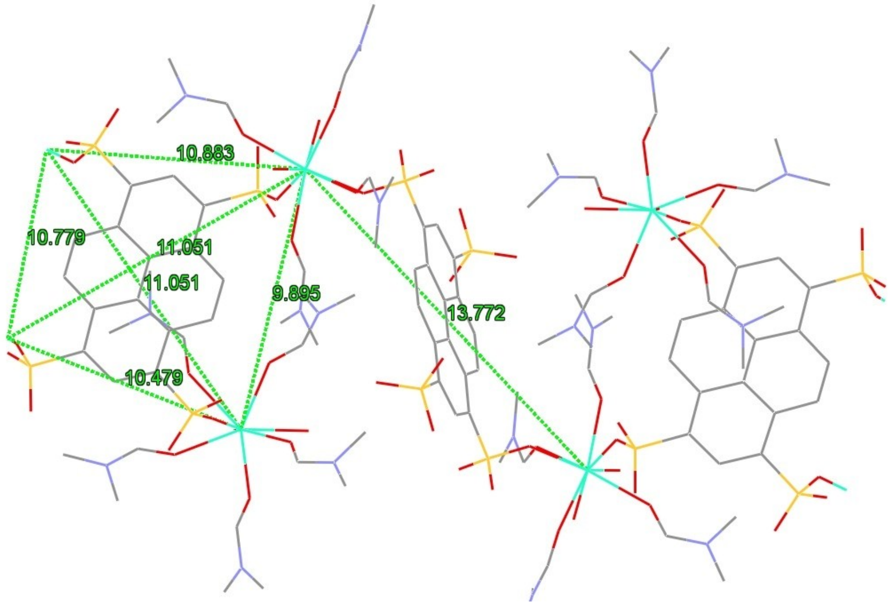

Figure S2. Diferent Dy···Dy distances through the *pytet* ligand that exhibits two coordination modes.

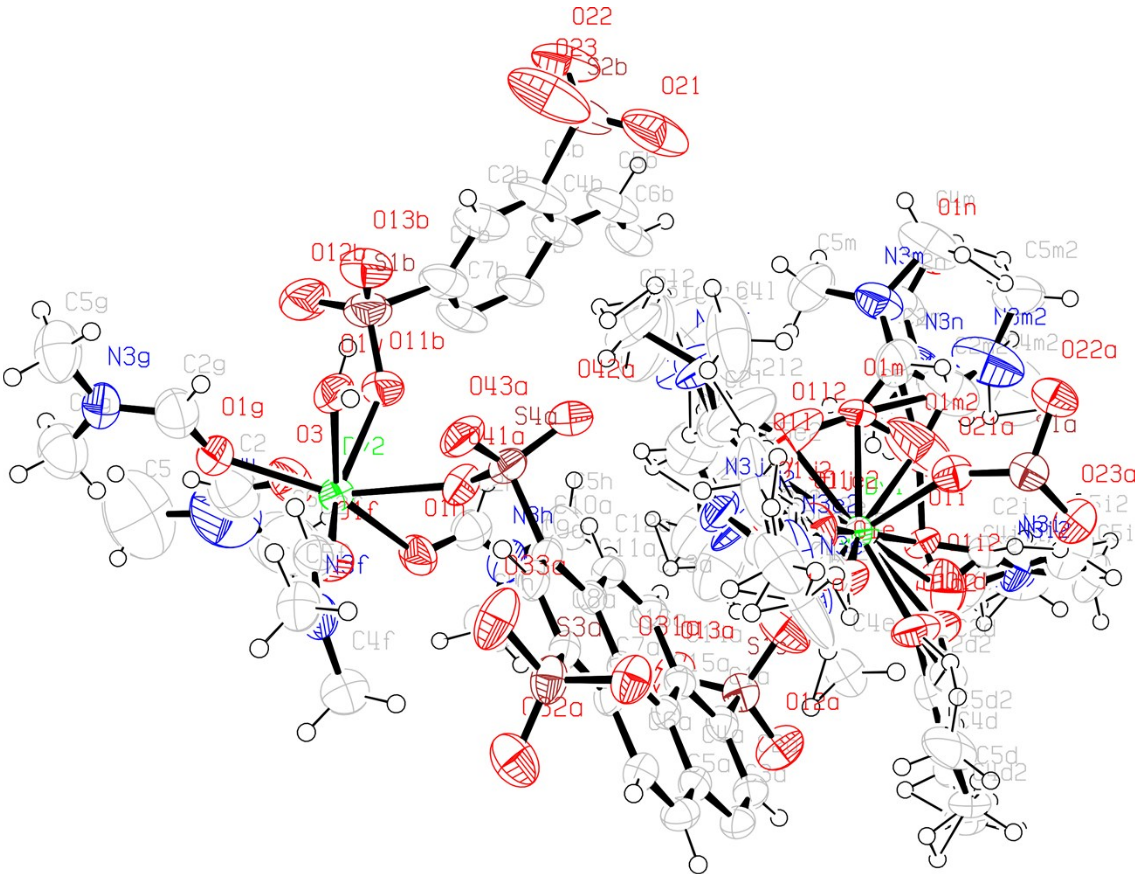

Figure S3. ORTEP view of the asymmetric unit of compound **1**.

2. Elemental analysis of pytet ligand

Elemental (C, H, N and S) analyses were performed on a Leco CHNS-932 microanalyzer, whereas the metal content (Dy for compound **1** and Na for pytet ligand) was determined by inductively coupled plasma (ICP-AES) on a Horiba Yobin Yvon Activa spectrometer.

Table S1. Elemental analyses of compound **1** and pytet ligand.

Compound	**C (%)**		**H (%)**		**N (%)**		**S (%)**		**M (%)**	
	Exp.	***Cal.***	***Exp.***	***Cal.***	***Exp.***	***Cal.***	***Exp.***	***Cal.***	***Exp.***	***Cal.***
$C_{60}H_{99}N_{12}O_{33}S_6Dy_2$										
Compound **1**	35.04	35.43	4.87	4.91	7.98	8.26	9.63	9.46	16.12	15.98
$C_{26}H_{28}N_3NaO_{17}S_4$										
Pytet ligand	34.55	34.75	3.32	3.14	4.74	4.68	13.98	14.29	12.74	12.80

3. Continuous Shape Measurements

Table S2. Continuous Shape Measurements for compound **1**.

OP-8	D8h	Octagon
HPY-8	C7v	Heptagonal pyramid
HBPY-8	D6h	Hexagonal bipyramid
CU-8	Oh	Cube
SAPR-8	D4d	Square antiprism
TDD-8	D2d	Triangular dodecahedron
JGBF-8	D2d	Johnson gyrobifastigium J26
JETBPY-8	D3h	Johnson elongated triangular bipyramid J14
JBTPR-8	C2v	Biaugmented trigonal prism J50
BTPR-8	C2v	Biaugmented trigonal prism
JSD-8	D2d	Snub diphenoid J84
TT-8	Td	Triakis tetrahedron
ETBPY-8	D3h	Elongated trigonal bipyramid

	OP-8	HPY-8	HBPY-8	CU-8	SAPR-8	**TDD-8**	JGBF-8
Dy1	32.057	24.073	13.921	11.240	2.307	**1.033**	11.121
Dy2	30.007	24.162	16.694	9.882	1.222	**0.708**	14.017

	JETBPY-8	JBTPR-8	BTPR-8	JSD-8	TT-8	ETBPY-8
Dy1	28.497	2.362	2.166	2.564	11.937	24.193
Dy2	29.086	1.637	1.251	2.645	10.432	25.082

4. Powder X-ray Diffraction

X-ray powder diffraction (XRPD) pattern was collected on a Phillips X'PERT powder diffractometer with Cu-Kα radiation (λ = 1.54060 Å) over the $5 < 2\theta < 50^{\circ}$ range with a step size of 0.026º and an acquisition time of 5 s per step at 25 ºC. A fixed divergence slit was employed for the experiment. Indexation of the diffraction profile was made by means of the FULLPROF program (pattern-matching analysis) on the basis of the space group and the cell parameters refined on single-crystal X-ray diffraction.

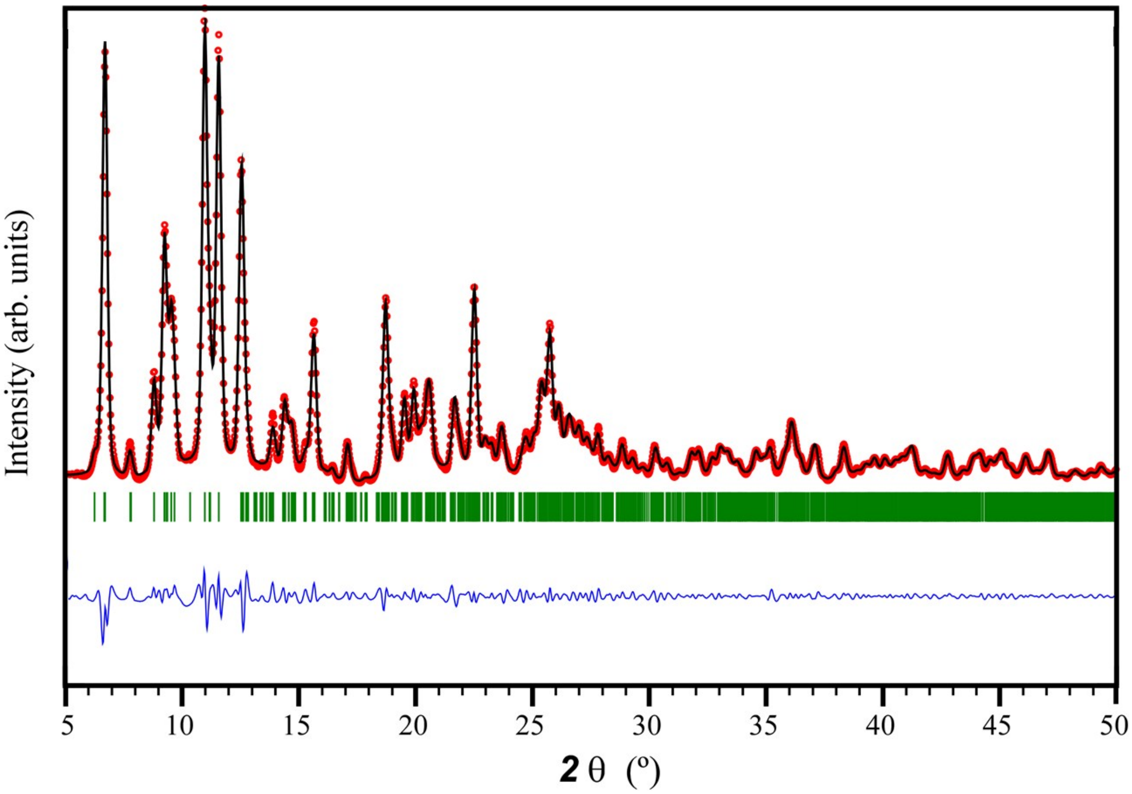

Figure S4. Pattern-matching refinement of compound **1**.

5. FT-IR analysis

FTIR spectra of powdered samples were recorded in the 400–4000 cm^{-1} region on a Nicolet 6700 FTIR spectrophotometer using KBr pellets. As inferred from Figure Sx, both spectra show a close resemblance containing bands attributed to C=C vibrations and aromatic C–H vibrations corresponding to pytet ligand. However, the band centered at 1600 cm^{-1} in the spectrum of *pytet* compound (with $[Na_5(\mu_3\text{-formato})(\mu_4\text{-pytet})(DMF)_3]_n$ formula) is clearly structured owing to the occurrence of formate ion in the compound. In particular, the shoulder peaking at 1610 cm^{-1} can be unequivocally attributed to the asymmetric vibration of O–C–O of formate ion, which is not present in compound **1**.

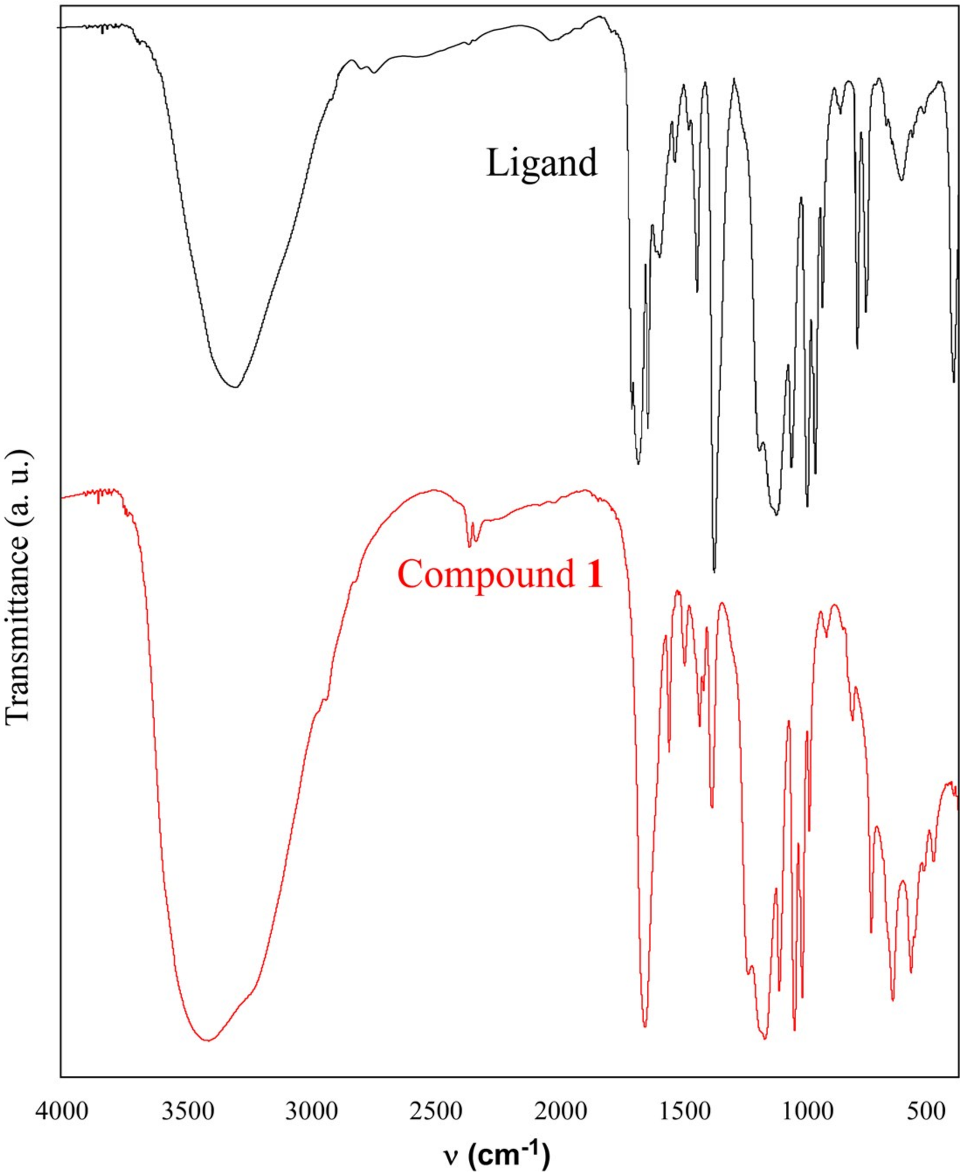

Figure S5. FTIR spectra of compounds **1** and pytet ligand.

Magnetic Properties

The anisotropy axis has been drawn for the crystallographically independent dysprosium(III) ions by using Magellan software developed by Chilton group. This software estimates the orientation of the magnetic anisotropy of the $m_J = \pm 15/2$ state of Dy^{III} via electrostatic optimation of the aspherical electron density distribution.

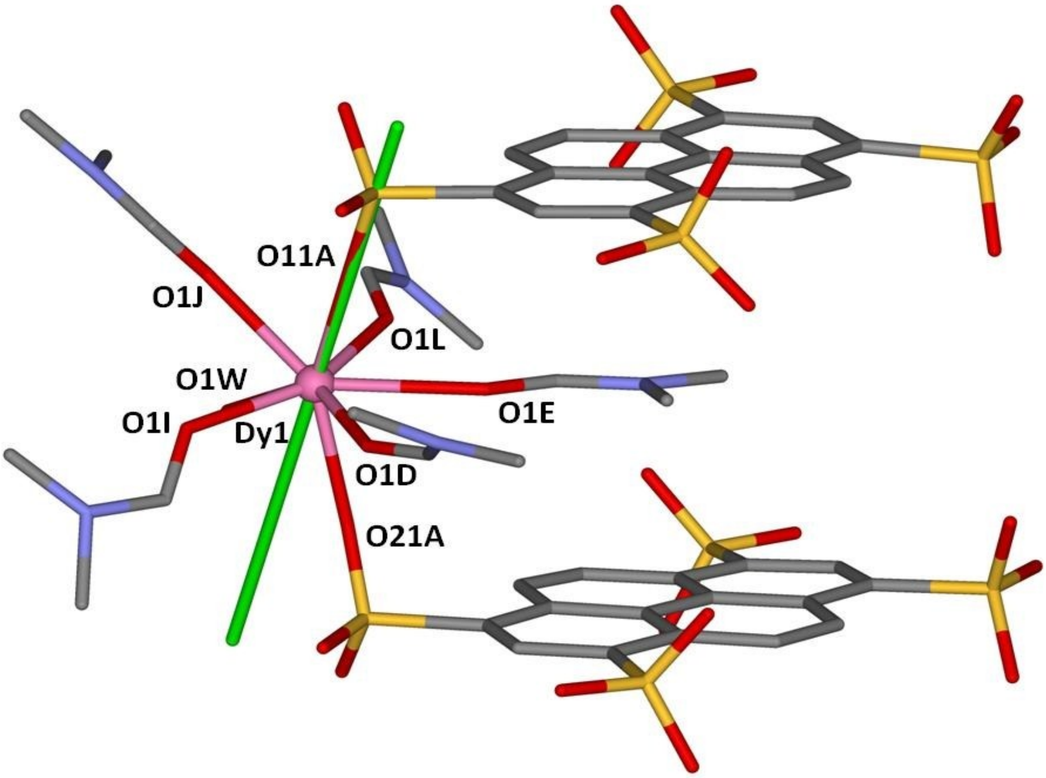

Bond	Distance (Å)	Bond	Distance (Å)
Dy1-O11A	2.290(7)	Dy1-O1I	2.211(12)
Dy1-O21A	2.306(6)	Dy1-O1J	2.313(9)
Dy1-O1D	2.264(11)	Dy1-O1L	2.307(19)
Dy1-O1E	2.472(12)	Dy1-O1W	2.365(12)

Figure S6. Orientation of the magnetic moment (green line) for Dy1 of complex **1**. Bottom: selected bond distances for complex **1**.

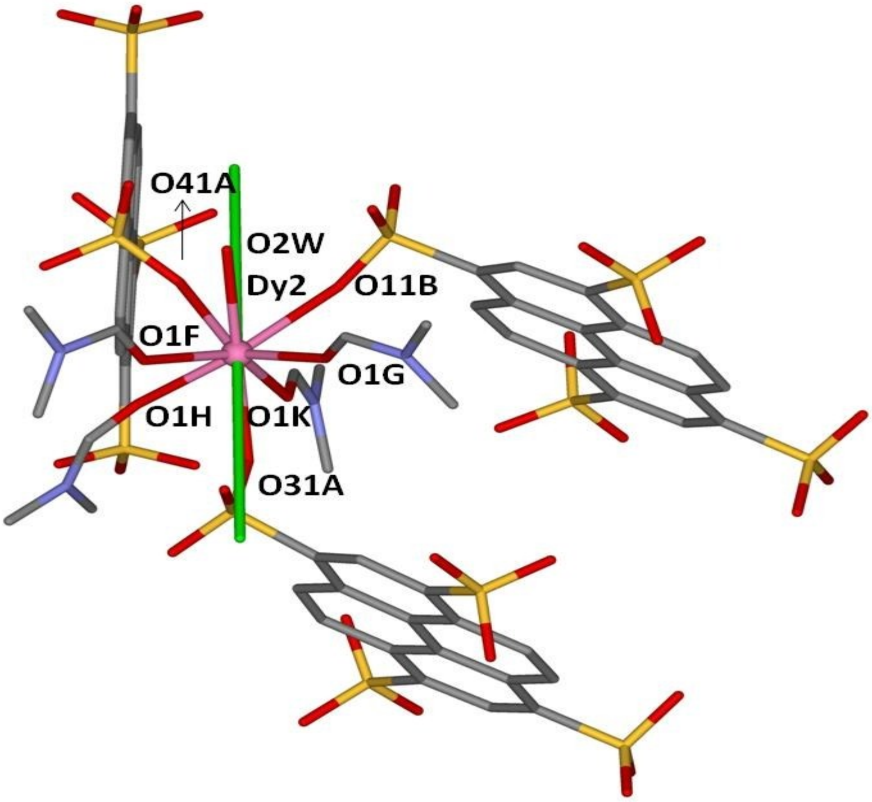

Bond	Distance (Å)	Bond	Distance (Å)
Dy2-31A	2.353(6)	Dy2-O1G	2.296(6)
Dy2-41A	2.415(6)	Dy2-O1H	2.342(6)
Dy2-11B	2.315(6)	Dy2-O1K	2.361(8)
Dy2-O1F	2.303(6)	Dy2-O2W	2.503(6)

Figure S7. Orientation of the magnetic moment (green line) for Dy2 of complex **1**. Bottom: selected bond distances for complex **1**.

Experimental Conditions:

Alternating current (*ac*) magnetic measurements were performed under zero and 1000 Oe applied static fields on a PPMS - Quantum Design Model 6000 magnetometer by using an oscillating *ac* field of 3.5 G and *ac* frequencies ranging from 60 to 10 000 Hz.

6. Photoluminescence Properties.

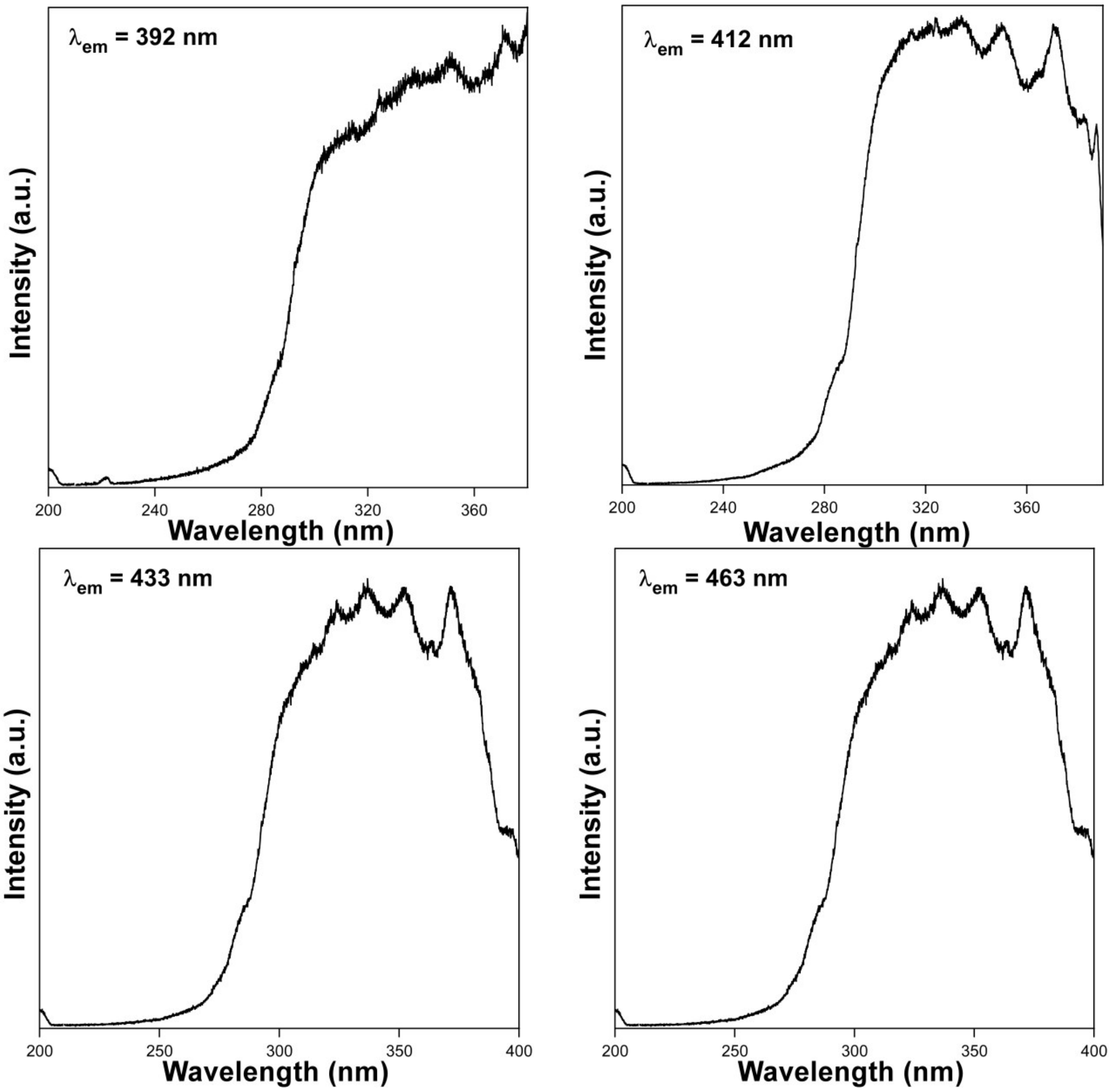

Figure S8. Excitation spectra at 10 K for compound **1**.

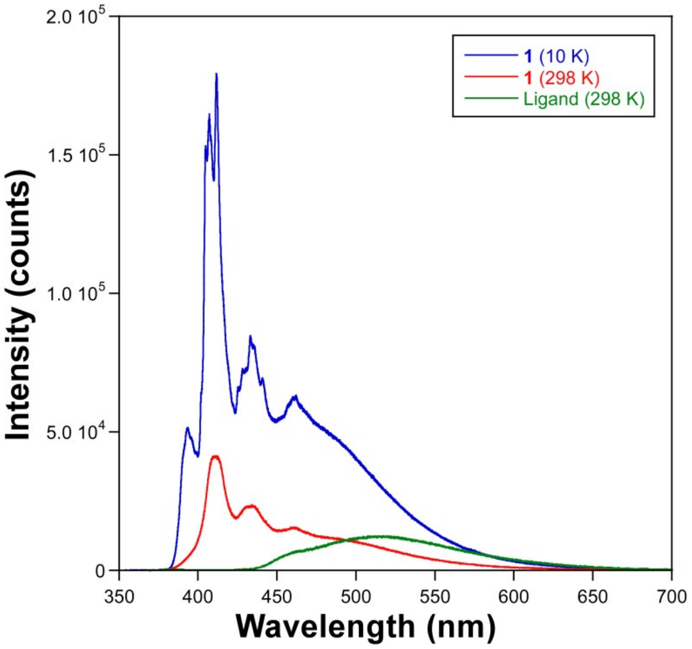

Figure S9. Emission spectra of compound **1** (at selected temperatures) and ligand recorded under the same conditions for comparative purposes.

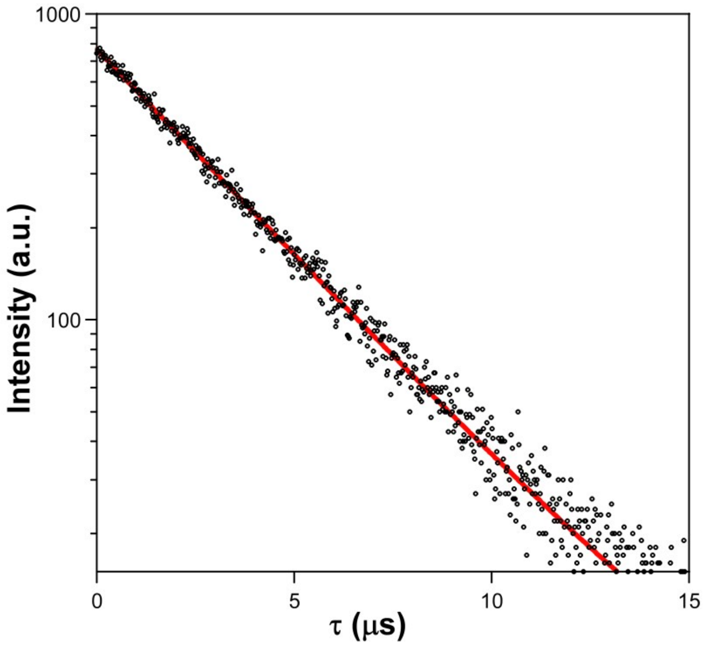

Figure S10. Emission decay curve (black circles) and fitting (red line) of compound **1** at 10 K.

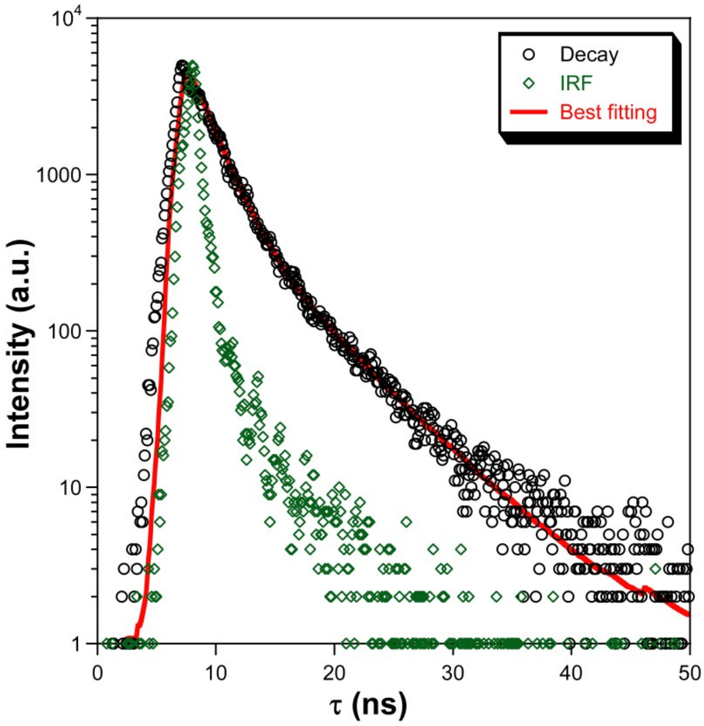

Figure S11. Emission decay curve (black circles) and fitting (red line) of ligand at 10 K.

Experimental Conditions:

Lifetime and steady state photoluminescence (PL) were measured on crystalline samples from 10 K to room temperature using a close cycle helium cryostat enclosed in an Edinburgh Instruments FLS920 spectrometer. For steady state measurements, an IK3552R-G HeCd continuous laser (325 nm) was used as the excitation source, whereas a Müller-Elektronik-Optik SVX1450 Xe lamp was employed to collect the excitation spectra. Photographs of irradiated single-crystal and polycrystalline samples were taken at room temperature in a micro-PL system included in an Olympus optical microscope illuminated with a HeCd laser or a Hg lamp.